Journal of
Mechanics of
Materials and Structures

SCALE EFFECTS ON ULTRASONIC WAVE DISPERSION
CHARACTERISTICS OF MONOLAYER GRAPHENE
EMBEDDED IN AN ELASTIC MEDIUM

Saggam Narendar and Srinivasan Gopalakrishnan

msp

SCALE EFFECTS ON ULTRASONIC WAVE DISPERSION CHARACTERISTICS OF MONOLAYER GRAPHENE EMBEDDED IN AN ELASTIC MEDIUM

SAGGAM NARENDAR AND SRINIVASAN GOPALAKRISHNAN

Ultrasonic wave propagation in a graphene sheet, which is embedded in an elastic medium, is studied using nonlocal elasticity theory incorporating small-scale effects. The graphene sheet is modeled as an one-atom thick isotropic plate and the elastic medium/substrate is modeled as distributed springs. For this model, the nonlocal governing differential equations of motion are derived from the minimization of the total potential energy of the entire system. After that, an ultrasonic type of wave propagation model is also derived. The explicit expressions for the cut-off frequencies are also obtained as functions of the nonlocal scaling parameter and the y-directional wavenumber. Local elasticity shows that the wave will propagate even at higher frequencies. But nonlocal elasticity predicts that the waves can propagate only up to certain frequencies (called escape frequencies), after which the wave velocity becomes zero. The results also show that the escape frequencies are purely a function of the nonlocal scaling parameter. The effect of the elastic medium is captured in the wave dispersion analysis and this analysis is explained with respect to both local and nonlocal elasticity. The simulations show that the elastic medium affects only the flexural wave mode in the graphene sheet. The presence of the elastic matrix increases the band gap of the flexural mode. The present results can provide useful guidance for the design of next-generation nanodevices in which graphene-based composites act as a major element.

1. Introduction

Graphene [Geim and Novoselov 2007], the two-dimensional (2D) counterpart of three-dimensional (3D) graphite, has attracted vast interest in solid-state physics, materials science, and nanoelectronics since it was discovered in 2004 as the first free-standing 2D crystal. Graphene is considered a promising electronic material in postsilicon electronics. However, large-scale synthesis of high-quality graphene represents a bottleneck for next-generation graphene devices. Existing routes for graphene synthesis include mechanical exfoliation of highly ordered pyrolytic graphite [Novoselov et al. 2004], eliminating Si from the surface of single-crystal SiC [Ohta et al. 2006], depositing graphene at the surface of single-crystal [Oshima and Nagashima 1997] or polycrystalline metals [Obraztsov et al. 2007], and various wet-chemistry-based approaches [Gómez-Navarro et al. 2007; Li et al. 2008]. However, up to now no methods have delivered high quality graphene with the large area required for applications such as practical electronic materials. In recent years, these nanostructured materials have spurred considerable interest in the materials community because of their potential for large gains in mechanical and physical properties as compared to standard structural materials. Since controlled experiments in nanoscale are

difficult and molecular dynamics simulations are expensive and formidable, especially for large scale systems, modified continuum models have been widely and successfully used to study the mechanical behavior of nanostructures like carbon nanotubes (CNTs), graphene sheets (GSs), nanofibers/wires, etc. [Tomanek and Enbody 2000].

A nanostructure is defined as a material system or object where at least one of the dimensions is below 100 nm. Oxide nanostructures can be classified into three categories: zero-dimensional (0D); one-dimensional (1D); and two-dimensional (2D). 0D nanostructures are materials in which all three dimensions are at the nanoscale. Good examples of these materials are buckminsterfullerenes [Kroto et al. 1985] and quantum dots [Dabbousi et al. 1997]. 1D nanostructures are materials that have two physical dimensions in the nanometer range while the third dimension can be large, such as in CNTs [Vossen and Kern 1978]. 2D nanostructures, or thin films, only have one dimension in the nanometer range and can be used readily in the processing of complimentary metal-oxide semiconductor transistors [Senturia 2001] and microelectromechanical systems [Martin 1996]. Since the focus of this work is on 2D nanostructures, the others will not be discussed from this point forward. 2D nanostructures (here graphene sheets) have stimulated a great deal of interest due to their importance in fundamental scientific research and potential technological applications in the development of GS-based nanodevices such as strain sensors, mass and pressure sensors, atomic dust detectors, enhancers of surface image resolution, etc.

In contrast to the investigations of CNTs, it is surprising to find that very few studies have been reported in the literature on the theoretical modeling of GSs, even though graphene possesses many superior properties [Luo and Chung 2000], such as good electrical and thermal conductivities parallel to the sheets and poor conductivities normal to the sheets, which makes it suitable for gasket material in high-temperature or chemical environments; good flexibility, which suggests its use as a vibration damping material; and a high strength-to-weight ratio, which makes it an ideal material for sports equipment. Recently, Behfar and Naghdabadi [2005] investigated the nanoscale vibration of a multilayered graphene sheet (MLGS) embedded in an elastic medium, in which the natural frequencies as well as the associated modes were determined using a continuum-based model. The influence of carbon-carbon and carbon-polymer van der Waals (VDW) forces are considered in their work. They further studied the bending modulus of a MLGS using a geometrically based analytical approach [Behfar et al. 2006]. The bending energy in their analysis is based on the VDW interactions of atoms belonging to two neighboring sheets. Their calculations are performed for a double-layered GS, but the derived bending modulus is generalized to a MLGS composed of many double-layered GSs along its thickness, in which the double-layered GSs are alternately the same in configuration. In addition, it should be mentioned that graphite is composed of multilayered sheets, but it was recently reported [Horiuchi et al. 2004] that single-layered sheets are detectable in carbon nanofilms. Sakhaee-Pour et al. [2008a] have studied the free vibrational behavior of single-layer graphene sheets (SLGS) while considering the effects of chirality and aspect ratio as well as boundary conditions, and have developed predictive models for computing the natural frequencies. The potential applications of SLGSs as mass sensors and atomistic dust detectors have further been investigated [Sakhaee-Pour et al. 2008b]. Also, the promising usage of SLGSs as strain sensors has been examined [Sakhaee-Pour and Ahmadian 2008].

The small scale of nanotechnology makes the applicability of classical and local continuum models, such as beam and shell models, questionable. Classical continuum models do not admit intrinsic size

dependence in the elastic solutions of inclusions and inhomogeneities. At nanometer scales, however, size effects often become prominent, the cause of which needs to be explicitly addressed due to an increasing interest in the general area of nanotechnology [Li et al. 2008]. Sun and Zhang (see [Tomanek and Enbody 2000]) indicated the importance of semicontinuum models in analyzing nanomaterials after pointing out the limitations of the applicability of classical continuum models to nanotechnology. In their semicontinuum model for nanostructured materials with plate-like geometry, the material properties were found to be completely dependent on the thickness of the plate structure, contrary to classical continuum models. The modeling of such a size-dependent phenomenon has become an interesting research subject in this field [Vossen and Kern 1978; Kroto et al. 1985; Dabbousi et al. 1997]. It is thus concluded that the applicability of classical continuum models at very small scales is questionable, since the material microstructure, such as the lattice spacing between individual atoms, becomes increasingly important at small sizes and the discrete structure of the material can no longer be homogenized into a continuum. Therefore, continuum models need to be extended to consider the scale effect in nanomaterial studies.

At nanometer scales, size effects often become prominent. Both experimental and atomistic simulation results have shown a significant size-effect in the mechanical properties when the dimensions of these structures become small. As the length scales are reduced, the influences of long-range interatomic and intermolecular cohesive forces on the static and dynamic properties tend to be significant and cannot be neglected. The classical theory of elasticity, being the long wave limit of atomic theory, excludes these effects. Thus traditional classical continuum mechanics would fail to capture small-scale effects when dealing in nanostructures. Small-size analysis using local theory over predicts the results. Thus the consideration of small effects is necessary for correct prediction of micro/nanostructures. Various size-dependent continuum theories which capture the small scale parameter such as couple-stress elasticity theory [Zhou and Li 2001], strain gradient theory [Fleck and Hutchinson 1997], and modified couple-stress theory [Yang et al. 2002] have been reported. These modified continuum theories are being used for the analysis of small-scale structures. However, the most used continuum theory for analyzing small-scale structures is Eringen's nonlocal elasticity theory [Eringen 1972; 1976; 1983; Eringen and Edelen 1972]. The essence of nonlocal elasticity theory is that the small-scale effects are captured by assuming that the stress at a point is a function of the strains at all the other points in the domain. Nonlocal theory considers long-range interatomic interaction and yields results dependent on the size of a body. It is also reported in [Chen et al. 2004] that nonlocal continuum theory-based models are physically reasonable from the atomistic viewpoint of lattice dynamics and molecular dynamics simulations. Understanding the importance of employing nonlocal elasticity theory in small-scale structures, a number of research works have conducted static, dynamic, and stability analyses of micro/nanostructures [Yakobson et al. 1997; Peddieson et al. 2003; Wang 2005; Wang and Hu 2005; Lu et al. 2006; 2007; Duan and Wang 2007; Duan et al. 2007; Ece and Aydoydu 2007; Lim and Wang 2007; Lu 2007; Reddy 2007; Wang and Liew 2007; Adali 2008; Kumar et al. 2008; Reddy and Pang 2008; Tounsi et al. 2008; Wang and Duan 2008; Yang et al. 2008; Aydogdu 2009a; 2009b; Murmu and Pradhan 2009; Narendar and Gopalakrishnan 2009a; 2009b; 2010a; 2010b; 2010c; 2010d; Narendar et al. 2010].

All engineering materials possess intrinsic length scales in terms of their repetitive atomic or molecular structures. The classical theory of elasticity, which is commonly used to explain the behavior of these materials, however, does not accommodate any such scale. The absence of the length scale creates several discrepancies in the predictions of mechanical responses, for example, infinite stress fields near crack tips

or nondispersive wave behavior (constant wave speed, independent of frequency). This occurs in classical elasticity, according to which Rayleigh waves propagating on the surface of a semiinfinite isotropic elastic space are nondispersive in nature [Love 1944], whereas experiments and the atomic theory of lattices predict otherwise. These anomalies indicate the limitations of the classical theory of elasticity and stress the need for molecular dynamics (MD)-based simulations. However, modern practical problems are still intractable for MD-based analysis, even if the highest computing capabilities are at disposal. Hence, refinement of the existing continuum theory for the purpose of more realistic predictions seems to be the only viable alternative. Several attempts have been made so far in this direction, for example, the nonlocal theory of elasticity [Eringen 1972; 1976; 1983; Eringen and Edelen 1972], where the objective is always to modify the stress gradient term in the governing momentum equilibrium equations so that the long-range effects are taken into account. The nonlocal theory generates a singular perturbed partial differential equation. In this work, the nonlocal theory of Eringen is used to develop wave solutions for 2D nanostructures such as graphene. However, in this work, the main concern is the issues involved in wave propagation analysis in the domain of nonlocal elasticity.

One important outcome of the nonlocal elasticity is the realistic prediction of the dispersion curve, that is, the frequency-wavenumber/wavevector relation. As shown in [Eringen 1983], the dispersion relation

$$\frac{\omega}{C_1 k} = \left(1 + (e_0 a)^2 k^2\right)^{-1/2}, \tag{1}$$

where $e_0 a$ is the nonlocality parameter, closely matches with the Born–Karman model dispersion

$$\frac{\omega a}{C_1} = 2\sin\left(\frac{ka}{2}\right) \tag{2}$$

when $e_0 = 0.39$ is considered. However, among the two natural conditions at the midpoint and end of the first Brillouin zone:

$$\left.\frac{d\omega}{dk}\right|_{k=0} = C_1, \quad \left.\frac{d\omega}{dk}\right|_{k=\frac{\pi}{a}} = 0, \tag{3}$$

these relations satisfy only the first one. It has been suggested that two-parameter approximation of the kernel function will give better results. This is reiterated in [Lazar et al. 2006], that a one-parameter (only $e_0 a$) nonlocal kernel will never be able to model the lattice dynamics relation and it is necessary to use the bi-Helmholtz type equation with two different coefficients of nonlocality to satisfy all the boundary conditions.

The simple forms of the group and phase velocities that exist for isotropic materials allow us to tune the nonlocality parameters so that the lattice dispersion relation is matched. Further, by virtue of the Helmholtz decomposition, only the 1D Brillouin zone needs to be handled. Although the general form of the boundary conditions, that is, group speed is equal to phase speed (at $k = 0$) or zero (at $k = \pi/a$), is still applicable, the expressions are difficult to handle. This is because the Brillouin zone is really a 2D region where four boundary conditions are involved.

Wave propagation in GSs has been a topic of great interest in the nanomechanics of GSs, where the equivalent continuum models are widely used. In this manuscript, we examine this issue by incorporating the nonlocal theory into the classical beam model. The influence of the nonlocal effects has been investigated in detail. The results are qualitatively different from those obtained based on the local beam

theory and thus are important for the development of GS-based nanodevices. The present work is an extension of [Sakhaee-Pour and Ahmadian 2008], in which we studied ultrasonic wave propagation in GS using nonlocal elasticity theory incorporating small-scale effects. The graphene was considered as free standing. In the present work, the unstable graphene is made stable by resting it on substrate. The substrate is assumed and modeled as an elastic medium. The present modeling and results can provide useful guidance for the design of next-generation nanodevices where graphene-based composites act as major elements. For a given nanostructure, the nonlocal small scale coefficient can be obtained by matching the results from MD simulations and the nonlocal elasticity calculations. At that value of the nonlocal scale coefficient, the waves will propagate in the nanostructure at that cut-off frequency. In the present paper, different values of e_0a are used. One can get the exact e_0a for a given GS by matching the MD simulation results of graphene with the results presented in this paper.

In the literature, there is no work on ultrasonic wave propagation in GSs with or without the effects of an elastic matrix. In the present paper, a nonlocal elasticity theory is used for analyzing ultrasonic wave propagation in GSs embedded in an elastic matrix. The present paper is organized as follows. In Section 2, Eringen's nonlocal elasticity theory is explained. In Section 3, the nonlocal governing partial differential equations are given for the graphene-elastic matrix system. Then ultrasonic wave propagation in graphene is carried out. Explicit expressions for the wavenumbers and group/phase speeds for the first three modes (in-plane-longitudinal, lateral, and flexural) of the wave are derived. The wave dispersion results are shown with and without elastic matrix effects. We also show that the flexural wave in graphene is highly affected by the presence of the elastic matrix. In Section 4, some important results are discussed in the context of the effects of nonlocality and the substrate. Finally, the paper ends with some important observations and conclusions.

2. Mathematical formulation

2.1. *A review of the theory of nonlocal elasticity.* The theory of nonlocal elasticity [Eringen 1972; 1976; 1983; Eringen and Edelen 1972] accommodates an equivalent effect due to nearest neighbor interaction and beyond the single lattice in the sense of lattice average stress and strain. This model considers that the stress state at a reference point $\mathbf{x}$ in the body is regarded to be dependent not only on the strain state at $\mathbf{x}$ but also on the strain states at all other points $\mathbf{x}'$ of the body. This is in accordance with the atomic theory of lattice dynamics and experimental observations on phonon dispersion. The most general form of the constitutive relation in the nonlocal elasticity-type representation involves an integral over the entire region of interest. The integral contains a nonlocal kernel function, which describes the relative influences of the strains at various locations on the stress at a given location. For nonlocal linear elastic solids, the equations of motion have the form

$$t_{ij,j} + f_i = \rho \ddot{u}_i, \tag{4}$$

where ρ and f_i are, respectively, the mass density and the body (and/or applied) forces; u_i is the displacement vector; and t_{ij} is the stress tensor of the nonlocal elasticity defined by

$$t_{ij}(\mathbf{X}) = \int_V \alpha(|\mathbf{X}' - \mathbf{X}|)\sigma_{ij}(\mathbf{X}')\,dv(\mathbf{X}'), \tag{5}$$

in which $\mathbf{X}$ is a reference point in the body; $\alpha(|\mathbf{X}' - \mathbf{X}|)$ is the nonlocal kernel function; and σ_{ij} is the local stress tensor of classical elasticity theory at any point $\mathbf{X}'$ in the body and satisfies the constitutive relations

$$\sigma_{ij} = c_{ijkl}\varepsilon_{kl}, \quad \varepsilon_{kl} = 0.5(u_{k,l} + u_{l,k}), \tag{6}$$

for a general elastic material, in which c_{ijkl} are the elastic modulus components with the symmetry properties $c_{ijkl} = c_{jikl} = c_{ijlk} = c_{klij}$, and ε_{kl} is the strain tensor. We stress that the boundary conditions involving tractions are based on the nonlocal stress tensor t_{ij} and not on the local stress tensor σ_{ij}.

The properties of the nonlocal kernel $\alpha(|\mathbf{X}' - \mathbf{X}|)$ have been discussed in detail in [Eringen 1983]. When $\alpha(|\mathbf{X}|)$ takes on a Green's function of a linear differential operator $\mathscr{L}$, that is,

$$\mathscr{L}\alpha(|\mathbf{X}' - \mathbf{X}|) = \delta(|\mathbf{X}' - \mathbf{X}|), \tag{7}$$

the nonlocal constitutive relation (5) is reduced to the differential equation

$$\mathscr{L}t_{ij} = \sigma_{ij} \tag{8}$$

and the integro-partial differential equation (4) is correspondingly reduced to the partial differential equation

$$\sigma_{ij} + \mathscr{L}(f_i - \rho\ddot{u}_i) = 0. \tag{9}$$

By matching the dispersion curves with lattice models, Eringen [1972; 1983; Eringen and Edelen 1972] proposed a nonlocal model with the linear differential operator $\mathscr{L}$ defined by

$$\mathscr{L} = 1 - (e_0 a)^2 \nabla^2, \tag{10}$$

where a is an internal characteristic length (lattice parameter, granular size, or molecular diameter) and e_0 is a constant appropriate to each material for adjusting the model to match some reliable results by experiments or other theories. Therefore, according to (6), (8), and (10), the constitutive relations may be simplified to

$$\left(1 - (e_0 a)^2 \nabla^2\right)t_{ij} = \sigma_{ij} = c_{ijkl}\varepsilon_{kl}. \tag{11}$$

For simplicity and to avoid solving integro-partial differential equations, the nonlocal elasticity model, defined by the relations (8)–(11), has been widely adopted for tackling various problems of linear elasticity and micro/nanostructural mechanics.

Generally used 3D and 2D nonlocal kernel functions are given the following equations, respectively,

$$\alpha(|\mathbf{X}|) = \frac{1}{4\pi\ell^2\tau^2|\mathbf{X}|}e^{-|\mathbf{X}|/\ell\tau}, \quad \alpha(|\mathbf{X}|) = \frac{1}{2\pi\ell^2\tau^2}K_0\left(\frac{|\mathbf{X}|}{\ell\tau}\right), \tag{12}$$

where $\tau = g/\ell$, K_0 is the modified Bessel function, and ℓ is a characteristic length of the considered structure.

Eringen [1983] proposed $e_0 = 0.39$ by the matching of the dispersion curves via nonlocal theory for plane waves and the Born-Karman model of lattice dynamics applied at the Brillouin zone boundary ($k = \pi/a$), where a is the distance between atoms and k is the wavenumber in the phonon analysis. On the other hand, Eringen and Edelen [1972] proposed $e_0 = 0.31$ for Rayleigh surface waves via nonlocal continuum mechanics and lattice dynamics. In the present paper, we assume that $e_0 = 0.39$ for analyzing ultrasonic wave propagation in an embedded monolayer graphene.

3. Ultrasonic wave characteristics of graphene embedded in an elastic matrix

3.1. *Derivation of nonlocal governing partial differential equations of motion.* In this section, we will derive the nonlocal governing differential equations of motion of the graphene-elastic substrate system.

For the present analysis we consider a single graphene layer resting on an elastic substrate (see Figure 1). This system is modeled as an one-atom thick nanoplate on distributed elastic springs. The displacement field is assumed as

$$u(x, y, z, t) = u^o(x, y, t) - z\frac{\partial w}{\partial x},$$
$$v(x, y, z, t) = v^o(x, y, t) - z\frac{\partial w}{\partial y}, \tag{13}$$
$$w(x, y, z, t) = w(x, y, t),$$

where $u^o(x, y, t)$, $v^o(x, y, t)$, and $w(x, y, t)$ are the axial (in-plane-longitudinal and lateral) and transverse displacements, respectively, along the midplane as shown in Figure 1. The midplane of the plate is at $z = 0$. The associated nonzero strains are obtained as

$$\begin{Bmatrix} \varepsilon_{xx} \\ \varepsilon_{yy} \\ \varepsilon_{xy} \end{Bmatrix} = \begin{Bmatrix} \dfrac{\partial u^o}{\partial x} \\ \dfrac{\partial v^o}{\partial y} \\ \dfrac{\partial u^o}{\partial y} + \dfrac{\partial v^o}{\partial x} \end{Bmatrix} + \begin{Bmatrix} -\dfrac{\partial^2 w}{\partial x^2} \\ -\dfrac{\partial^2 w}{\partial y^2} \\ -2\dfrac{\partial^2 w}{\partial x \partial y} \end{Bmatrix}, \tag{14}$$

where ε_{xx} and ε_{yy} are the normal strains in the x and y directions, respectively, while, ε_{xy} is the in-plane shear strain.

The nonlocal constitutive relation for isotropic materials is given as

$$\begin{Bmatrix} \sigma_{xx} \\ \sigma_{yy} \\ \sigma_{xy} \end{Bmatrix} - (e_0 a)^2 \left(\frac{\partial^2}{\partial x^2} + \frac{\partial^2}{\partial y^2} \right) \begin{Bmatrix} \sigma_{xx} \\ \sigma_{yy} \\ \sigma_{xy} \end{Bmatrix} = \begin{bmatrix} C_{11} & \nu C_{11} & 0 \\ \nu C_{22} & C_{22} & 0 \\ 0 & 0 & C_{66} \end{bmatrix} \begin{Bmatrix} \varepsilon_{xx} \\ \varepsilon_{yy} \\ \varepsilon_{xy} \end{Bmatrix}, \tag{15}$$

where σ_{xx} and σ_{yy} are the normal stresses in the x and y directions, respectively, and σ_{xy} is the in-plane shear stress. For the case of an isotropic plate, the expressions for C_{ij} in terms of the Young's modulus E and Poisson's ratio ν are given as $C_{11} = C_{22} = E/(1 - \nu^2)$ and $C_{66} = E/(2(1 + \nu))$.

The total strain energy (Π) and kinetic energy (Γ) are calculated as

$$\Pi = \frac{1}{2} \int_{-h/2}^{+h/2} \int_A (\sigma_{xx}\varepsilon_{xx} + \sigma_{yy}\varepsilon_{yy} + \sigma_{xy}\varepsilon_{xy} + 2K^{\text{elastic}} w^2) \, dz \, dA, \tag{16}$$

$$\Gamma = \frac{1}{2} \int_{-h/2}^{+h/2} \int_A \rho(\dot{u}^2 + \dot{v}^2 + \dot{w}^2) \, dz \, dA. \tag{17}$$

Substituting (14) and (15) in (16) and (17) and using Hamilton's principle,

$$\int_{t_1}^{t_2} (\delta\Pi - \delta\Gamma) \, dt = 0, \tag{18}$$
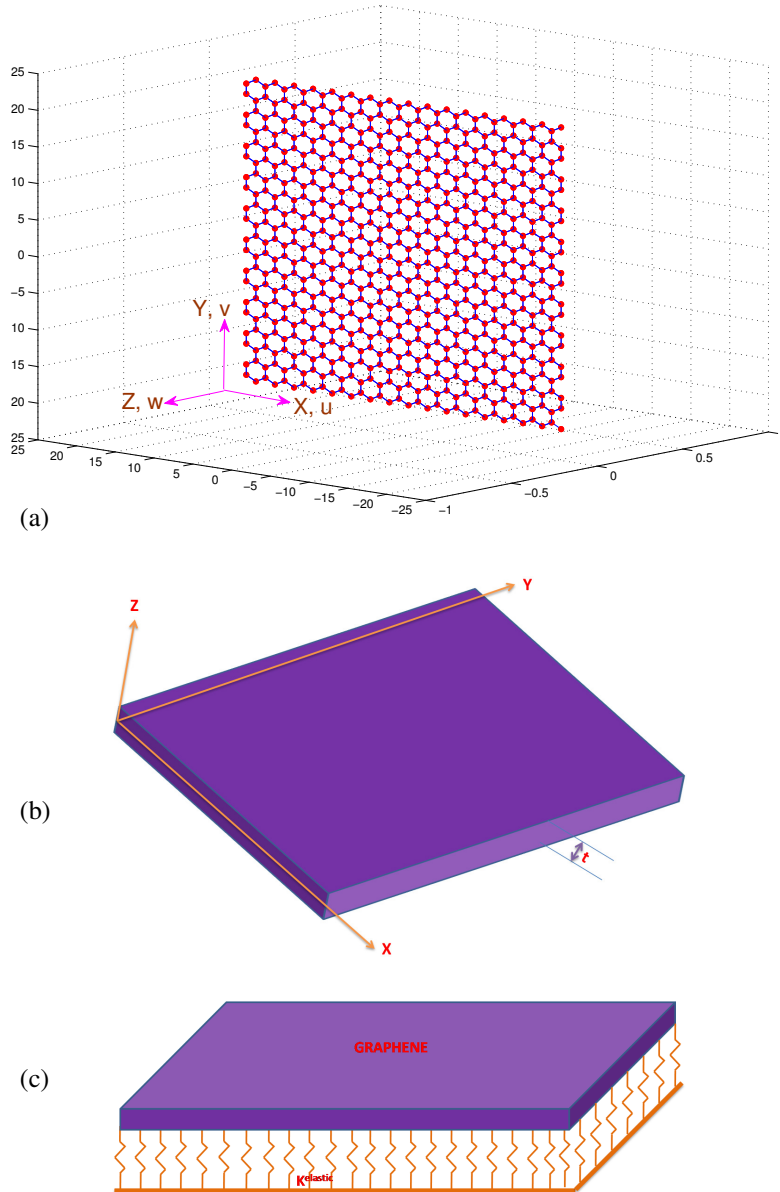
Figure 1. Single-layered GS: (a) discrete model (a monolayer graphene of $40\,\text{Å} \times 40\,\text{Å}$, consisting of 680 carbon atoms arranged in hexagonal array), (b) equivalent continuum model, and (c) continuum equivalent model of monolayer graphene embedded in an elastic medium, where K^{elastic} denotes the modulus parameter of the surrounding medium.

the minimization of the strain and kinetic energies with respect to the three degrees of freedom (u^o, v^o, w) will give three governing partial differential equations for the assumed system (graphene embedded in

matrix) as

$$\delta u^o: \quad -J_0\frac{\partial^2 u^o}{\partial t^2} + J_0(e_0 a)^2\left(\frac{\partial^4 u^o}{\partial x^2 \partial t^2} + \frac{\partial^4 u^o}{\partial y^2 \partial t^2}\right) - I_0\left(C_{11}\frac{\partial^2 u^o}{\partial x^2} + C_{66}\frac{\partial^2 u^o}{\partial y^2}\right) + I_0(C_{12}+C_{66})\frac{\partial^2 v^o}{\partial x \partial y}$$
$$+ J_1\frac{\partial^3 w}{\partial x \partial t^2} - J_1(e_0 a)^2\left(\frac{\partial^5 w}{\partial x^3 \partial t^2} + \frac{\partial^5 w}{\partial x \partial y^2 \partial t^2}\right) - C_{11}I_1\frac{\partial^3 w}{\partial x^3} - I_1(C_{12}+2C_{66})\frac{\partial^3 w}{\partial x \partial y^2} = 0, \quad (19)$$

$$\delta v^o: \quad -J_0\frac{\partial^2 v^o}{\partial t^2} + J_0(e_0 a)^2\left(\frac{\partial^4 v^o}{\partial x^2 \partial t^2} + \frac{\partial^4 v^o}{\partial y^2 \partial t^2}\right) - I_0\left(C_{22}\frac{\partial^2 v^o}{\partial y^2} + C_{66}\frac{\partial^2 v^o}{\partial x^2}\right) + I_0(C_{12}+C_{66})\frac{\partial^2 u^o}{\partial x \partial y}$$
$$+ J_1\frac{\partial^3 w}{\partial y \partial t^2} - J_1(e_0 a)^2\left(\frac{\partial^5 w}{\partial x^2 \partial y \partial t^2} + \frac{\partial^5 w}{\partial y^3 \partial t^2}\right) - C_{22}I_1\frac{\partial^3 w}{\partial y^3} - I_1(C_{12}+2C_{66})\frac{\partial^3 w}{\partial x^2 \partial y} = 0, \quad (20)$$

$$\delta w: \quad -J_0\frac{\partial^2 w}{\partial t^2} + J_2\left(\frac{\partial^4 w}{\partial x^2 \partial t^2} + \frac{\partial^4 w}{\partial y^2 \partial t^2}\right) + J_0(e_0 a)^2\left(\frac{\partial^4 w}{\partial x^2 \partial t^2} + \frac{\partial^4 w}{\partial y^2 \partial t^2}\right)$$
$$- J_2(e_0 a)^2\left(\frac{\partial^6 w}{\partial x^4 \partial t^2} + 2\frac{\partial^6 w}{\partial x^2 \partial y^2 \partial t^2} + \frac{\partial^6 w}{\partial y^4 \partial t^2}\right) + 2K^{\text{elastic}}(e_0 a)^2\left(\frac{\partial^2 w}{\partial x^2} + \frac{\partial^2 w}{\partial y^2}\right)$$
$$- 2K^{\text{elastic}} w - I_2\left(C_{11}\frac{\partial^4 w}{\partial x^4} + C_{22}\frac{\partial^4 w}{\partial y^4}\right) - 2I_2(C_{11}+2C_{66})\frac{\partial^4 w}{\partial x^2 \partial y^2} - J_1\frac{\partial^3 u^o}{\partial x \partial t^2}$$
$$+ J_1(e_0 a)^2\left(\frac{\partial^5 u^o}{\partial x^3 \partial t^2} + \frac{\partial^5 u^o}{\partial x \partial y^2 \partial t^2}\right) + C_{11}I_1\frac{\partial^3 u^o}{\partial x^3} + I_1(C_{12}+2C_{66})\frac{\partial^3 u^o}{\partial x \partial y^2}$$
$$- J_1\frac{\partial^3 v^o}{\partial y \partial t^2} + J_1(e_0 a)^2\left(\frac{\partial^5 v^o}{\partial x^2 \partial y \partial t^2} + \frac{\partial^5 v^o}{\partial y^3 \partial t^2}\right) + I_1(C_{12}+2C_{66})\frac{\partial^3 v^o}{\partial x^2 \partial y} + C_{22}I_1\frac{\partial^3 v^o}{\partial y^3} = 0, \quad (21)$$

where K^{elastic} is the force constant of the bond between the GS and the elastic matrix and

$$I_p = \int_{-h/2}^{h/2} z^p\, dz, \quad J_p = \int_{-h/2}^{h/2} \rho z^p\, dz, \quad p = 0, 1, 2. \quad (22)$$

If the nonlocal scaling parameter $e_0 a$ is zero, then the above three governing differential equations of motion become classical governing equations.

3.2. *Ultrasonic wave dispersion and band gap analysis.* For harmonic wave propagation in a GS, the displacement field can be written in complex form as [Zhou and Li 2001]

$$u^o(x, y, t) = \hat{u}e^{-jk_x x}e^{-jk_y y}e^{j\omega t},$$
$$v^o(x, y, t) = \hat{v}e^{-jk_x x}e^{-jk_y y}e^{j\omega t}, \quad (23)$$
$$w^o(x, y, t) = \hat{w}e^{-jk_x x}e^{-jk_y y}e^{j\omega t},$$

where $\hat{u}$, $\hat{v}$, and $\hat{w}$ are the frequency amplitudes, k_x and k_y are the wavenumbers in the x and y-directions, respectively, ω is the frequency of the wave motion, and $j = \sqrt{-1}$.

The nonlocal governing partial differential equations of the graphene embedded in an elastic matrix model are given in (19)–(21). The next step is to analyze the ultrasonic type of wave propagation in these GSs. For this, substitute the displacement assumed as a harmonic type given in (23) in the governing

partial differential equations of the graphene and write the resultant equations in matrix form as (for nontrivial solutions of $\hat{u}$, $\hat{v}$, and $\hat{w}$)

$$\mathbf{S}_4 k_x^4 + \mathbf{S}_3 k_x^3 + \mathbf{S}_2 k_x^2 + \mathbf{S}_1 k_x + \mathbf{S}_0 = 0, \tag{24}$$

where

$$
\mathbf{S}_4 = \begin{bmatrix} 0 & 0 & 0 \\ 0 & 0 & 0 \\ 0 & 0 & J_2(e_0a)^2\omega^2 - C_{11}I_2 \end{bmatrix},
$$

$$
\mathbf{S}_3 = \begin{bmatrix} 0 & 0 & jJ_1\omega^2(e_0a)^2 - jC_{11}I_1 \\ 0 & 0 & 0 \\ -jJ_1\omega^2(e_0a)^2 + jC_{11}I_1 & 0 & 0 \end{bmatrix},
$$

$$
\mathbf{S}_2 = \begin{bmatrix} J_0\omega^2(e_0a)^2 - C_{11}I_0 & 0 & 0 \\ 0 & J_0\omega^2(e_0a)^2 - C_{66}I_0 & S_2^{(23)} \\ 0 & S_2^{(32)} & S_2^{(33)} \end{bmatrix}, \tag{25}
$$

$$
\mathbf{S}_1 = \begin{bmatrix} 0 & -(C_{11}+C_{66})I_0 k_y & S_1^{(13)} \\ -(C_{11}+C_{66})I_0 k_y & 0 & 0 \\ S_1^{(31)} & 0 & 0 \end{bmatrix},
$$

$$
\mathbf{S}_0 = \begin{bmatrix} S_0^{(11)} & 0 & 0 \\ 0 & S_0^{(22)} & S_0^{(23)} \\ 0 & S_0^{(32)} & S_0^{(33)} \end{bmatrix},
$$

where the elements $S_r^{(pq)}$ ($p, q = 1, 2, 3$ and $r = 0, 1, 2$) are given in the Appendix.

Equation (24) is in the form of polynomial eigenvalue problem in wavenumber k_x and is solved for the wavenumbers. This method is very generalized and efficient. The resulting wavenumbers are functions of wave frequency and are shown in Figures 2 and 3, obtained from both local and nonlocal elasticities, with and without the effect of the elastic matrix, respectively. The figures also show the effect of the substrate on the ultrasonic wave characteristics of graphene at $k_y = 0$, 2, and 5 nm^{-1}. In the wavenumber dispersion curves, the frequency at which the imaginary part of the wavenumber becomes real is called the frequency band gap region (0 to ω_c). The expressions for the frequency band gap are obtained by setting $k_x = 0$ in dispersion relation, (24). For the present case of a polynomial eigenvalue problem (PEP) one can solve Det($\mathbf{S}_0$) = 0 as

$$\omega_c^{\text{in-plane}} = k_y \sqrt{\frac{I_0 C_{66}}{J_0(1+(e_0a)^2 k_y^2)}}, \quad \omega_c^{\text{flexural}} = \sqrt{\frac{1}{2H_0}\sqrt{H_1+H_2}}, \tag{26}$$

where H_0, H_1, and H_2 are given in the Appendix.

The frequency band gap ($0 - \omega_c$, cut-off frequency) for all the fundamental modes (longitudinal, lateral, and flexural) for $k_y \neq 0$ in graphene with and without substrate effect. These cut-off frequencies are functions of the material properties of graphene, the y-direction wavenumber k_y, and the nonlocal scaling parameter e_0a.
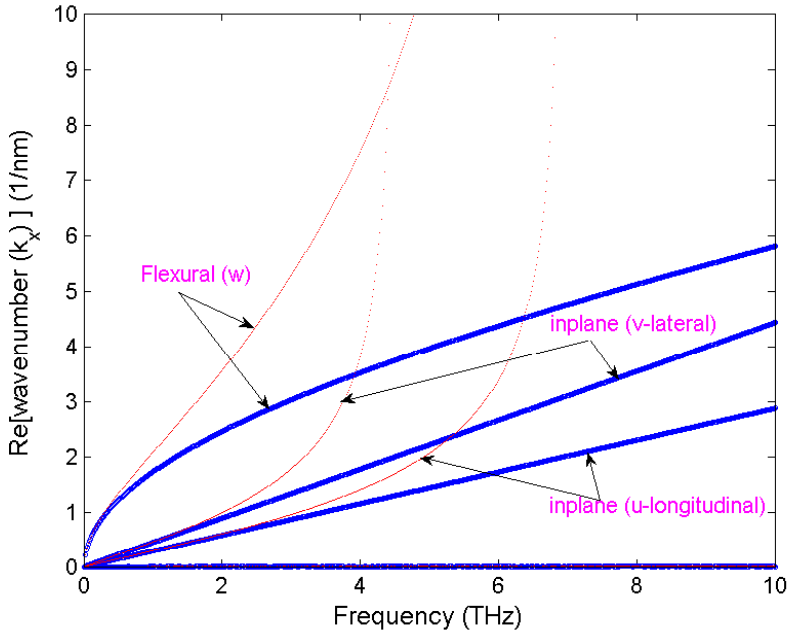
Figure 2. Wavenumber dispersion with wave frequency in the GS without considering the elastic matrix obtained from the local and nonlocal elasticity; here the y-directional wavenumber $k_y = 0$ and the nonlocal scaling parameter is $e_0 a = 0.5$ nm.
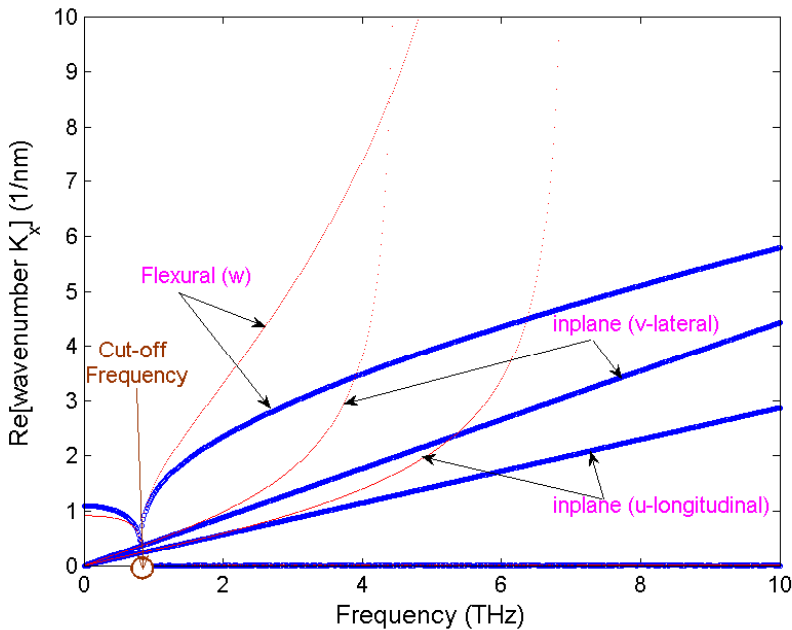
Figure 3. Wavenumber dispersion with wave frequency in the GS with considering the elastic matrix obtained from the local and nonlocal elasticity; here the y-directional wavenumber $k_y = 0$ and the nonlocal scaling parameter is $e_0 a = 0.5$ nm.

In the present work, it has been observed that the nonlocal scale parameter introduces a certain band gap region in the in-plane and flexural wave modes where no wave propagation occurs. This is manifest in the wavenumber plots as the region where the wavenumber tends to infinity or the wave speed tends to zero. The frequency at which this phenomenon occurs is called the *escape frequency*. The escape frequencies are obtained by solving $\mathrm{Det}(\mathbf{S}_4) = 0$. It can be noticed that $\mathbf{S}_4$ is singular, thus the lambda matrix $\Phi(k_x) = \mathbf{S}_4 k_x^4 + \mathbf{S}_3 k_x^3 + \mathbf{S}_2 k_x^2 + \mathbf{S}_1 k_x + \mathbf{S}_0$ is not regular [Fleck and Hutchinson 1997] and admits infinite eigenvalues [Yang et al. 2002]. So, the escape frequencies of these fundamental wavemodes can also obtained by substituting $k_x \to \infty$ in the expanded dispersion relation, (24), that is, a polynomial in k_x, and solving for the frequencies. The obtained escape frequencies of these three fundamental wave modes are

$$\omega_e^{\text{longitudinal}} = \frac{1}{e_0 a}\sqrt{\frac{C_{11}I_2}{J_2}}, \quad \omega_e^{\text{lateral}} = \frac{1}{e_0 a}\sqrt{\frac{C_{66}I_0}{J_0}}, \quad \omega_e^{\text{flexural}} = \frac{1}{e_0 a}\sqrt{\frac{C_{11}I_0}{J_0}}. \tag{27}$$

Here the suffix e represents the escape frequency. It can be seen that the escape frequencies are purely functions of the nonlocal scaling parameter and are not affected by the dimensions of the GS. Also, the escape frequencies are independent of the effect of the elastic matrix.

The wave speeds (phase speed $C_p = \omega/k_x$ and group speed $C_g = \partial\omega/\partial k_x$) can be computed from (24).

We differentiate the PEP with respect to wave frequency, to get a PEP in terms of group speed as

$$\mathbf{G}_1 C_g + \mathbf{G}_0 = 0, \tag{28}$$

where

$$\mathbf{G}_1 = \left[k_x^4 \frac{\partial \mathbf{S}_4}{\partial \omega} + k_x^3 \frac{\partial \mathbf{S}_3}{\partial \omega} + k_x^2 \frac{\partial \mathbf{S}_2}{\partial \omega} + k_x \frac{\partial \mathbf{S}_1}{\partial \omega} + \frac{\partial \mathbf{S}_0}{\partial \omega} \right],$$
$$\mathbf{G}_0 = 4\mathbf{S}_4 k_x^3 + 3\mathbf{S}_3 k_x^2 + 2\mathbf{S}_2 k_x + \mathbf{S}_1, \tag{29}$$

where $C_g = (\partial\omega/\partial k_x)$ is the group speed of waves in the graphene and the matrices $\mathbf{S}_4$, $\mathbf{S}_3$, $\mathbf{S}_2$, $\mathbf{S}_1$, and $\mathbf{S}_0$ are given in (25). This is also a PEP, and one can solve it for the group speeds (as a function of wave frequency, wavenumbers, and nonlocal scaling parameter) of respective modes (that is, for in-plane-u, v, and flexural-w) of the graphene.

We will discuss the phase speed dispersion with wave frequency, as shown in Figures 4–7, obtained from both local and nonlocal elasticity and taken with and without the effect of the elastic matrix. The phase speed dispersion shown is for both with and without the elastic matrix effects at $k_y = 0$ and $2\,\text{nm}^{-1}$.

3.3. *Numerical experiments, results and discussion.* For the present analysis, the Young's modulus of the graphene is taken as $1.06\,\text{TPa}$, the density is $2300\,\text{kg/m}^3$, and the size $40 \times 40\,\text{Å}$. The stiffness of the bond between the graphene and the matrix is $0.2694\,\text{N/m}$ and this has to be divided by the number of atoms per unit area of the graphene (38×10^{18}).

The wavenumber dispersion with wave frequency in the graphene without and with the elastic matrix, respectively, are shown in Figures 2 and 3, obtained from both the local and nonlocal elasticity. Figure 2 shows the wavenumber dispersion obtained from the local and nonlocal elasticity theory (where $e_0 a = 0$ and $e_0 a = 0.5\,\text{nm}$). Figures 2 and 3 are shown for $k_y = 0$ (which represents 1D wave propagation). In Figures 8 and 9 were have $k_y = 2\,\text{nm}^{-1}$. The frequency band gap of the flexural waves is small
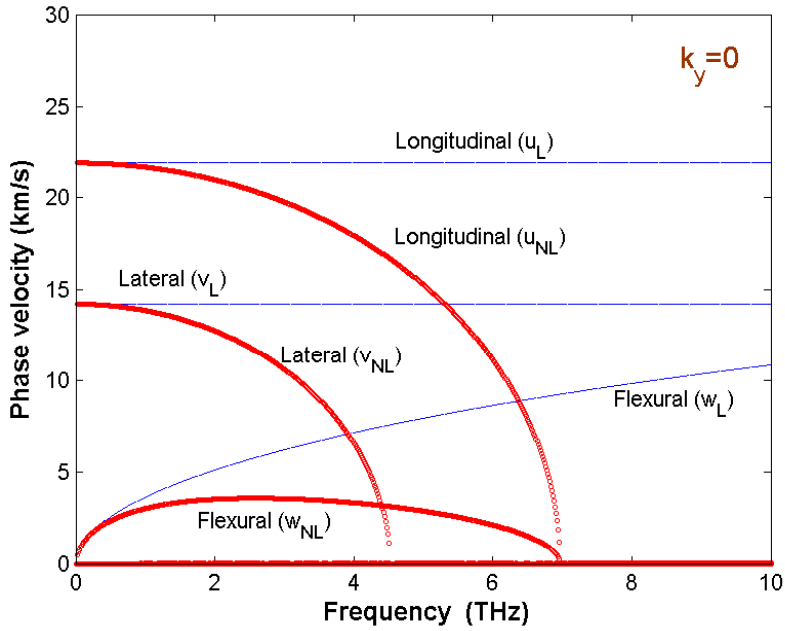
Figure 4. Phase velocity dispersion with wave frequency in the GS without considering the elastic matrix obtained from the local and nonlocal elasticity; here the y-directional wavenumber $k_y = 0$ and the nonlocal scaling parameter is $e_0 a = 0.5$ nm.
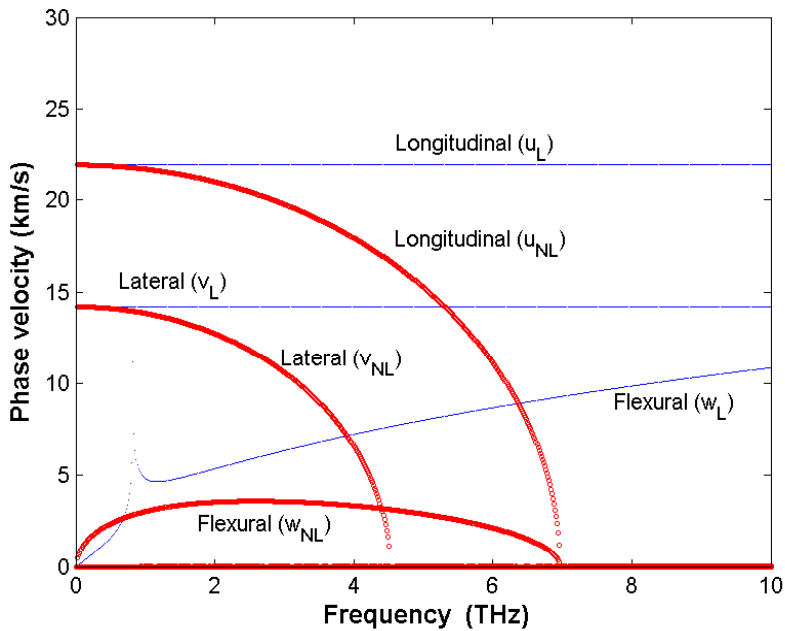
Figure 5. Phase velocity dispersion with wave frequency in the GS with considering the elastic matrix obtained from the local and nonlocal elasticity; here the y-directional wavenumber $k_y = 0$ and the nonlocal scaling parameter is $e_0 a = 0.5$ nm.
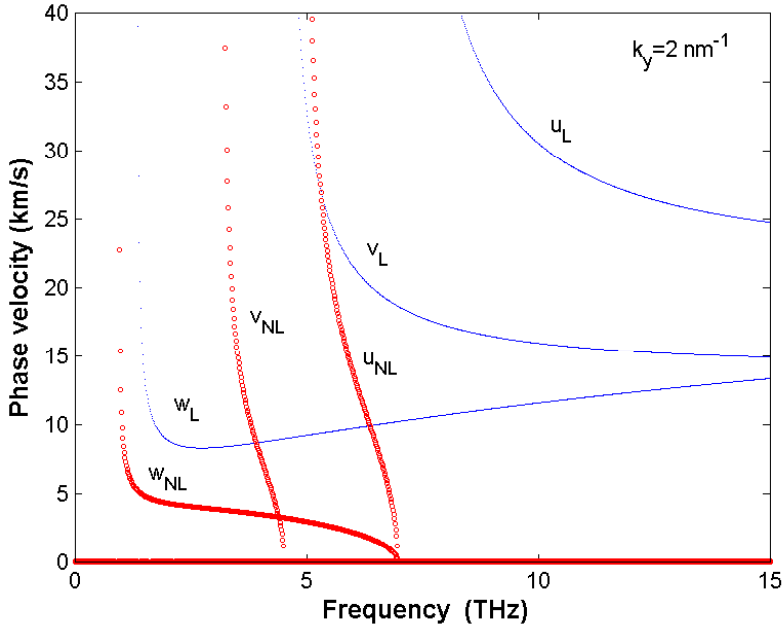
Figure 6. Phase velocity dispersion with wave frequency in the GS without considering the elastic matrix obtained from the local and nonlocal elasticity; here the y-directional wavenumber $k_y = 2\,\mathrm{nm}^{-1}$ and the nonlocal scaling parameter is $e_0 a = 0.5\,\mathrm{nm}$.
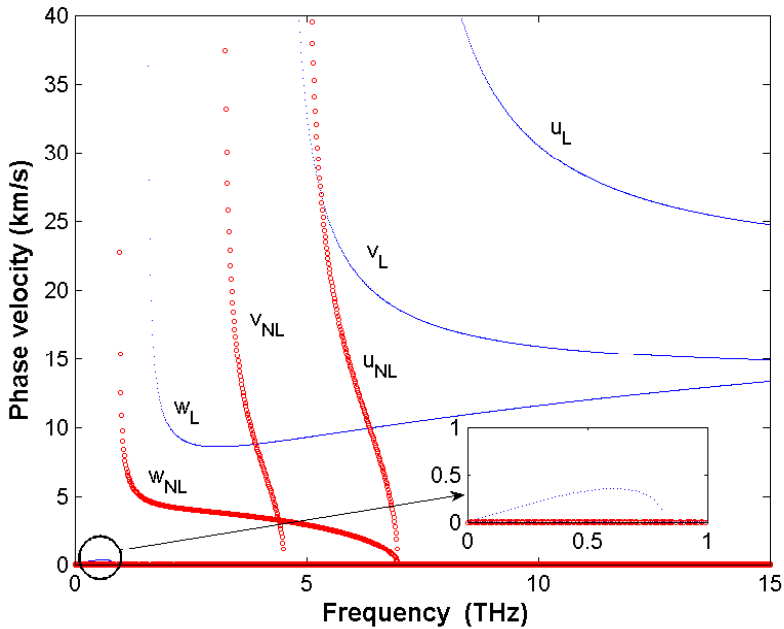
Figure 7. Phase velocity dispersion with wave frequency in the GS with considering the elastic matrix obtained from the local and nonlocal elasticity; here the y-directional wavenumber $k_y = 2\,\mathrm{nm}^{-1}$ and the nonlocal scaling parameter is $e_0 a = 0.5\,\mathrm{nm}$.
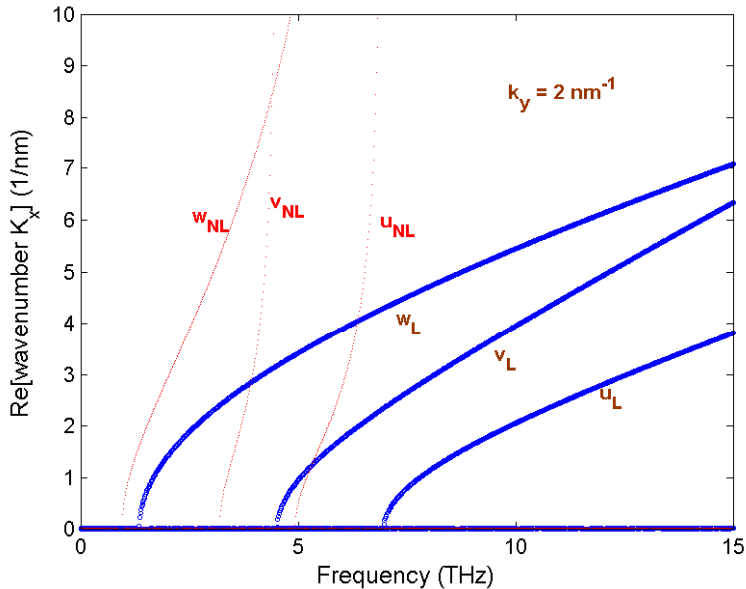
Figure 8. Wavenumber dispersion with wave frequency in the GS without considering the elastic matrix obtained from the local and nonlocal elasticity; here the y-directional wavenumber $k_y = 2 \, \text{nm}^{-1}$ and the nonlocal scaling parameter is $e_0 a = 0.5 \, \text{nm}$.

as compared to that of the longitudinal and lateral (in-plane) waves for the case without the elastic matrix effect. As the y-directional wavenumber k_y increases the frequency band gap of all the three fundamental modes increases. If we consider the elastic matrix effect, then the flexural wave starts propagating after a high-frequency band gap as compared to that of no matrix effect. The local elasticity shows a linear variation of the axial wavenumbers with frequency for $k_y = 0$, that is, the longitudinal and lateral wavenumbers are nondispersive in nature. For $k_y = 0$ the flexural wavenumber shows a nonlinear variation at low values of wave frequency; at higher values of wave frequency it varies linearly as shown in Figure 2. As k_y increases all the wavenumbers are dispersive in nature. In Figures 3 and 9 one can observe the matrix effect on flexural waves.

Wavenumber dispersion with frequency for nonlocal elasticity ($e_0 a = 0.5 \, \text{nm}$) is shown in Figures 2–9. The observations made for local elasticity are still valid for nonlocal elasticity. The only difference is that because of nonlocal elasticity the wavenumbers (for both in-plane and flexural) become highly nonlinear at higher wave frequencies. The frequency band gap variation is the same as we move from local to nonlocal elasticity with and without the elastic matrix effects.

Local elasticity shows that the wave will propagate even at higher frequencies. But nonlocal elasticity predicts that the waves can only propagate up to certain frequencies (called escape frequencies), after which it will stand, that is, there will be no propagation. The wavenumber dispersion curves obtained for nonlocal elasticity are shown up to the nonlocal limit only. The phenomena discussed at the beginning of this paragraph occurs above the nonlocal limit.

Phase speed dispersion with the wave frequency is shown in Figures 4–7 for local and nonlocal elasticity, for y-directional wavenumbers of $k_y = 0$ and $k_y = 2 \, \text{nm}^{-1}$. Figure 4 shows that (for $k_y = 0$) the
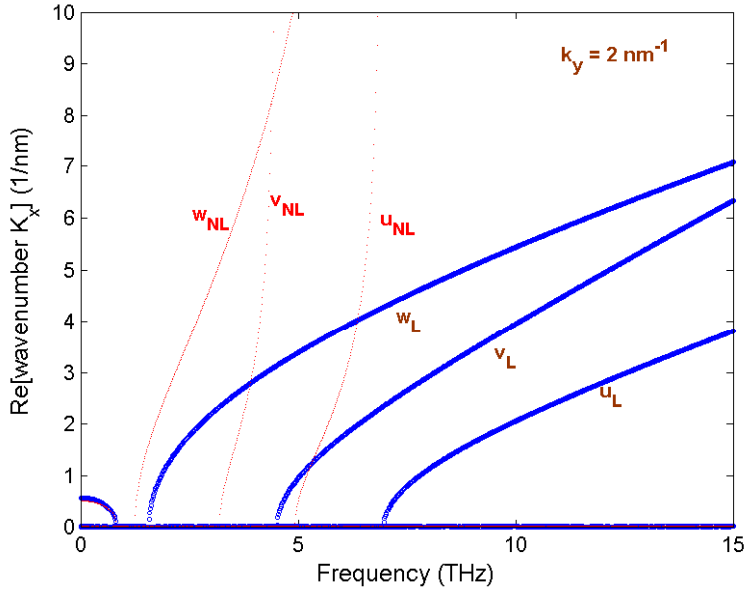
Figure 9. Wavenumber dispersion with wave frequency in the GS with considering the elastic matrix obtained from the local and nonlocal elasticity; here the y-directional wavenumber $k_y = 2\,\mathrm{nm}^{-1}$ and the nonlocal scaling parameter is $e_0 a = 0.5\,\mathrm{nm}$.

in-plane (u, v) wave speeds are constant with wave frequency, while flexural wave speeds increase from low frequency, after which they are constant for higher values of wave frequency. The magnitudes of the flexural phase speeds are higher compared to the axial wave group speeds. As k_y increases from 0 to $2\,\mathrm{nm}^{-1}$ the axial/in-plane wave speeds also show a dispersive nature. We can also observe the effect of the elastic matrix on the flexural wave phase speeds.

As we move to nonlocality, the phase speeds of the in-plane and flexural waves stop propagating at certain frequencies as shown in Figures 4–7. The phase speeds of the in-plane waves are the same for with or without the elastic matrix effect. The effect is only on the flexural wave speeds. There are two cut-off frequencies for the flexural waves with substrate effects from nonlocal elasticity. As k_y increases the flexural wave speeds retain the shape shown for local elasticity and the extra frequency band gap also vanishes.

From these results we can observe that only flexural waves are affected by the elastic matrix whether under local or nonlocal elasticity.

The variation of the cut-off frequencies of in-plane and flexural waves is shown in Figures 10 and 11, without and with the elastic matrix effect, respectively, and with y-directional wavenumbers of $k_y = 0, 2$ and $5\,\mathrm{nm}^{-1}$. The figures show that as we increase the nonlocal scaling parameter the cut-off frequencies of all the fundamental wave modes will decrease. For a given $e_0 a$, as we increase the y-directional wavenumber, the cut-off frequencies will increase. Because of the matrix, only the flexural wave mode cut-off frequencies are affected, as can be clearly seen from Figures 10 and 11.

The variation of the escape frequency with the nonlocal scaling parameter is shown in Figure 12. It can be seen that the escape frequencies of the longitudinal and flexural wave modes have equal values, and the latter wave has lower escape frequencies compared to that of longitudinal/flexural waves.
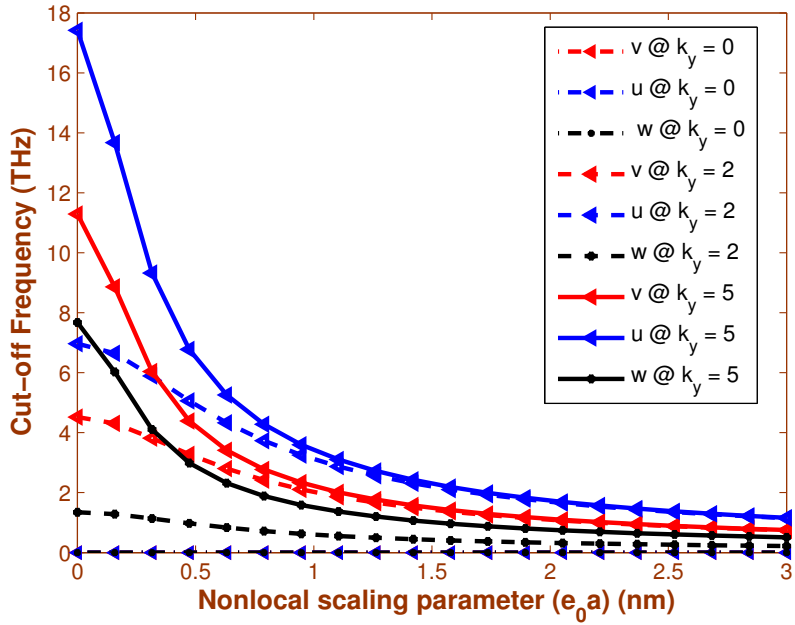
Figure 10. Cut-off frequency variation of longitudinal, lateral, and flexural waves obtained from the local and nonlocal elasticity without considering the effect of the matrix; k_y are in $1/nm$.
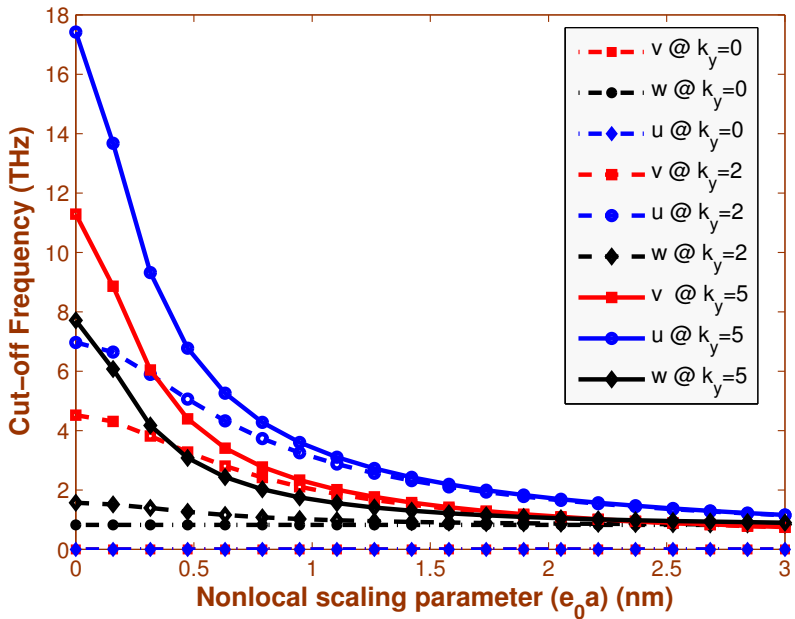
Figure 11. Cut-off frequency variation of longitudinal, lateral, and flexural waves obtained from the local and nonlocal elasticity with considering the effect of the matrix; k_y are in $1/nm$.
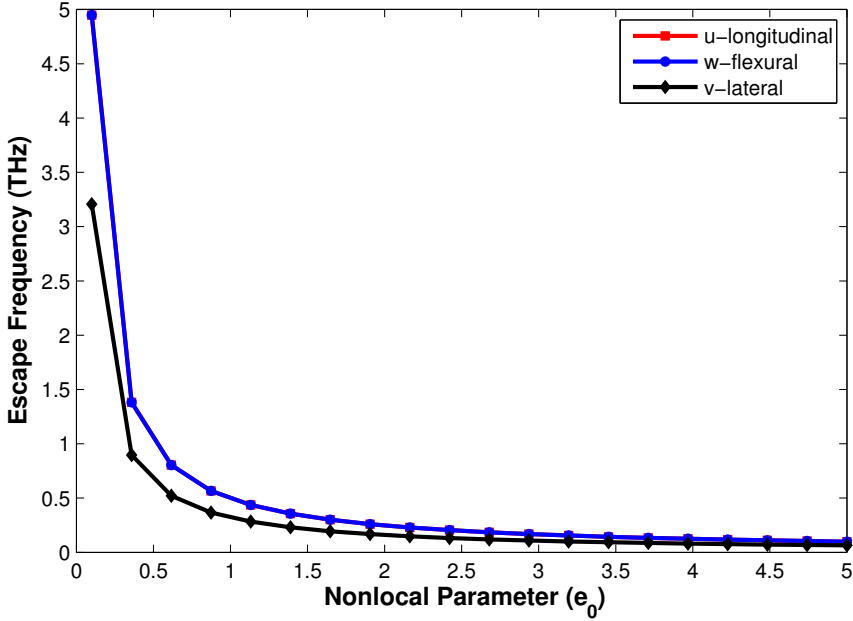
Figure 12. Cut-off frequency variation of longitudinal, lateral, and flexural waves obtained from the local and nonlocal elasticity with considering the effect of the matrix.

4. Conclusion

Ultrasonic wave propagation in a graphene sheet (GS), which is embedded in an elastic medium, was studied using a nonlocal elasticity theory incorporating small-scale effects. The GS was modeled as an one-atom thick isotropic plate and the elastic medium/substrate was modeled as distributed springs. For this model, the nonlocal governing differential equations of motion were derived from the minimization of the total potential energy of the entire system. After that, an ultrasonic type of wave propagation model was also derived. The explicit expressions for the cut-off and escape frequencies were also obtained as functions of the nonlocal scaling parameter and the y-directional wavenumber (k_y). The results of the wave dispersion analysis were shown for both local and nonlocal elasticity. From this analysis we showed that the elastic medium affected only the flexural wave mode in the GS. The present results can provide useful guidance for the design of next-generation nanodevices in which graphene-based composites act as major elements.

Appendix

Some of the elements of the matrices $[S_2]$, $[S_1]$, and $[S_0]$ are given in the following:

$$S_2^{(23)} = j J_1 k_y (e_0 a)^2 \omega^2 - j(C_{11} + 2C_{66}) I_1 k_y,$$
$$S_2^{(32)} = -j J_1 k_y (e_0 a)^2 \omega^2 + j(C_{11} + 2C_{66}) I_1 k_y,$$
$$S_2^{(33)} = J_2 \omega^2 \left(1 + (e_0 a)^2 k_y^2\right) - J_0 \omega^2 (e_0 a)^2 - (C_{11} + 2C_{66}) I_2 k_y^2 - K^{\text{elastic}} (e_0 a)^2;$$

$$S_1^{(13)} = jJ_1\omega^2\big(1 + (e_0a)^2k_y^2\big) - j(C_{11} + 2C_{66})I_1k_y^2,$$

$$S_1^{(31)} = -jJ_1\omega^2\big(1 + (e_0a)^2k_y^2\big) + j(C_{11} + 2C_{66})I_1k_y^2;$$

$$S_0^{(11)} = J_0\omega^2\big(1 + (e_0a)^2k_y^2\big) - C_{66}I_0k_y^2,$$

$$S_0^{(22)} = J_0\omega^2\big(1 + (e_0a)^2k_y^2\big) - C_{22}I_0k_y^2,$$

$$S_0^{(23)} = jJ_1k_y\omega^2\big(1 + (e_0a)^2k_y^2\big) - jC_{22}I_1k_y^3,$$

$$S_0^{(32)} = -jJ_1k_y\omega^2\big(1 + (e_0a)^2k_y^2\big) + jC_{22}I_1k_y^3,$$

$$S_0^{(33)} = J_2\omega^2k_y^2\big(1 + (e_0a)^2k_y^2\big) + J_0\omega^2\big(1 + (e_0a)^2k_y^2\big) - C_{22}I_2k_y^4 - K^{sub}\big(1 + (e_0a)^2k_y^2\big);$$

$$H_0 = (J_0J_2 - J_1^2)k_y^4(e_0a)^2 + J_0^2\big(1 + (e_0a)^2k_y^2\big) + (J_0J_2 - J_1^2)k_y^2,$$

$$H_1 = J_0K^{\text{elastic}}\big(1 + (e_0a)^2k_y^2\big) + (J_0 + J_2)C_{22}I_2k_y^4 + (I_0J_0 - 2I_1J_2)C_{22}k_y^4;$$

$$H_2 = [J_0^2(e_0a)^4k_y^4 + 2J_0^2(e_0a)^2k_y^2 + J_0^2]K^{\text{elastic}^2}\big[(2J_0^2I_2 - 2J_0I_0J_2 - 4J_0J_1I_1 + 4J_1^2I_0)C_{22}(e_0a)^2k_y^6$$

$$-\big(2J_0^2(e_0a)^2I_0 + 2J_0^2I_2 - 2J_0I_0J_2 - 4J_0J_1I_1 + 4J_1^2I_0\big)C_{22}k_y^4 - 2C_{22}I_0J_0^2k_y^2\big]K^{\text{elastic}}$$

$$+[J_0^2I_2^2 + I_0^2J_2^2 - 4J_0I_2J_1I_1 - 2J_0I_2I_0J_2 - 4J_1I_1I_0J_2 + 4J_0J_2I_1^2 + 4J_1^2I_0I_2]C_{22}^2k_y^8$$

$$+[4J_0^2I_1^2 - 2J_0^2I_2I_0 - 4I_0J_0J_1I_1 + 2I_0^2J_0J_2]C_{22}^2k_y^6 + I_0^2J_0^2C_{22}^2k_y^4.$$

References

[Adali 2008] S. Adali, "Variational principles for multi-walled carbon nanotubes undergoing buckling based on nonlocal elasticity theory", *Phys. Lett. A* **372**:35 (2008), 5701–5705.

[Aydogdu 2009a] M. Aydogdu, "Axial vibration of the nanorods with the nonlocal continuum rod model", *Physica E* **41**:5 (2009), 861–864.

[Aydogdu 2009b] M. Aydogdu, "A general nonlocal beam theory: its application to nanobeam bending, buckling and vibration", *Physica E* **41**:9 (2009), 1651–1655.

[Behfar and Naghdabadi 2005] K. Behfar and R. Naghdabadi, "Nanoscale vibrational analysis of a multi-layered graphene sheet embedded in an elastic medium", *Compos. Sci. Technol.* **65**:7–8 (2005), 1159–1164.

[Behfar et al. 2006] K. Behfar, P. Seifi, R. Naghdabadi, and J. Ghanbari, "An analytical approach to determination of bending modulus of a multi-layered graphene sheet", *Thin Solid Films* **496**:2 (2006), 475–480.

[Chen et al. 2004] Y. Chen, J. D. Lee, and A. Eskandarian, "Atomistic viewpoint of the applicability of microcontinuum theories", *Int. J. Solids Struct.* **41**:8 (2004), 2085–2097.

[Dabbousi et al. 1997] B. O. Dabbousi, J. RodriguezViejo, F. V. Mikulec, J. R. Heine, H. Mattoussi, R. Ober, K. F. Jensen, and M. G. Bawendi, "(CdSe) ZnS core-shell quantum dots: synthesis and characterization of a size series of highly luminescent nanocrystallites", *J. Phys. Chem. B* **101** (1997), 9463–9475.

[Duan and Wang 2007] W. H. Duan and C. M. Wang, "Exact solutions for axisymmetric bending of micro/nanoscale circular plates based on nonlocal plate theory", *Nanotechnology* **18**:38 (2007), Article ID #385704.

[Duan et al. 2007] W. H. Duan, C. M. Wang, and Y. Y. Zhang, "Calibration of nonlocal scaling effect parameter for free vibration of carbon nanotubes by molecular dynamics", *J. Appl. Phys.* **101**:2 (2007), Article ID #024305.

[Ece and Aydoydu 2007] M. C. Ece and M. Aydoydu, "Nonlocal elasticity effect on vibration of in-plane loaded double-walled carbon nano-tubes", *Acta Mech.* **190** (2007), 185–195.

[Eringen 1972] A. C. Eringen, "Linear theory of nonlocal elasticity and dispersion of plane waves", *Int. J. Eng. Sci.* **10** (1972), 425–435.

[Eringen 1976] A. C. Eringen, *Continuum physics, IV: Polar and non-local field theories*, Academic Press, New York, 1976.

[Eringen 1983] A. C. Eringen, "On differential equations of nonlocal elasticity and solutions of screw dislocation and surface waves", *J. Appl. Phys.* **54**:9 (1983), 4703–4710.

[Eringen and Edelen 1972] A. C. Eringen and D. G. B. Edelen, "On nonlocal elasticity", *Int. J. Eng. Sci.* **10** (1972), 233–248.

[Fleck and Hutchinson 1997] N. A. Fleck and J. W. Hutchinson, "Strain gradient plasticity", *Adv. Appl. Mech.* **33** (1997), 295–361.

[Geim and Novoselov 2007] A. K. Geim and K. S. Novoselov, "The rise of graphene", *Nat. Mater.* **6**:3 (2007), 183–191.

[Gómez-Navarro et al. 2007] C. Gómez-Navarro, R. T. Weitz, A. M. Bittner, M. Scolari, A. Mews, M. Burghard, and K. Kern, "Electronic transport properties of individual chemically reduced graphene oxide sheets", *Nano Lett.* **7**:11 (2007), 3499–3503.

[Horiuchi et al. 2004] S. Horiuchi, T. Gotou, and M. Fujiwara, "Single graphene sheet detected in a carbon nanofilm", *Appl. Phys. Lett.* **84**:13 (2004), 2403–2405.

[Kroto et al. 1985] H. W. Kroto, J. R. Heath, S. C. O'Brien, R. F. Curl, and R. E. Smalley, "C_{60}: Buckminsterfullerene", *Nature* **318**:6042 (1985), 162–163.

[Kumar et al. 2008] D. Kumar, C. Heinrich, and A. M. Waas, "Buckling analysis of carbon nanotubes modeled using nonlocal continuum theories", *J. Appl. Phys.* **103**:7 (2008), Article ID #073521.

[Lazar et al. 2006] M. Lazar, G. A. Maugin, and E. C. Aifantis, "On a theory of nonlocal elasticity of bi-Helmholtz type and some applications", *Int. J. Solids Struct.* **43**:6 (2006), 1404–1421.

[Li et al. 2008] X. L. Li, X. R. Wang, L. Zhang, S. W. Lee, and H. J. Dai, "Chemically derived, ultrasmooth graphene nanoribbon semiconductors", *Science* **319**:5867 (2008), 1229–1232.

[Lim and Wang 2007] C. W. Lim and C. M. Wang, "Exact variational nonlocal stress modeling with asymptotic higher-order strain gradients for nanobeams", *J. Appl. Phys.* **101**:5 (2007), Article ID #054312.

[Love 1944] A. E. H. Love, *A treatise on the mathematical theory of elasticity*, 4th ed., Dover, New York, 1944.

[Lu 2007] P. Lu, "Dynamic analysis of axially prestressed micro/nanobeam structures based on nonlocal beam theory", *J. Appl. Phys.* **101**:7 (2007), Article ID #073504.

[Lu et al. 2006] P. Lu, H. P. Lee, C. Lu, and P. Q. Zhang, "Dynamic properties of flexural beams using a nonlocal elasticity model", *J. Appl. Phys.* **99**:7 (2006), Article ID #073510.

[Lu et al. 2007] P. Lu, H. P. Lee, C. Lu, and P. Q. Zhang, "Application of nonlocal beam models for carbon nanotubes", *Int. J. Solids Struct.* **44**:16 (2007), 5289–5300.

[Luo and Chung 2000] X. Luo and D. D. L. Chung, "Vibration damping using flexible graphite", *Carbon* **38**:10 (2000), 1510–1512.

[Martin 1996] C. R. Martin, "Membrane-based synthesis of nanomaterials", *Chem. Mater.* **8**:8 (1996), 1739–1746.

[Murmu and Pradhan 2009] T. Murmu and S. C. Pradhan, "Vibration analysis of nano-single-layered graphene sheets embedded in elastic medium based on nonlocal elasticity theory", *J. Appl. Phys.* **105**:6 (2009), Article ID #064319.

[Narendar and Gopalakrishnan 2009a] S. Narendar and S. Gopalakrishnan, "Nonlocal scale effects on wave propagation in multi-walled carbon nanotubes", *Comput. Mater. Sci.* **47**:2 (2009), 526–538.

[Narendar and Gopalakrishnan 2009b] S. Narendar and S. Gopalakrishnan, "Scale effects on wave propagation in carbon nanotubes", pp. 549–558 in *IISc Centenary International Conference and Exhibition on Aerospace Engineering* (*ICEAE*) (Bangalore, 2009), Indian Institute of Science, Bangalore, 2009.

[Narendar and Gopalakrishnan 2010a] S. Narendar and S. Gopalakrishnan, "Nonlocal scale effects on ultrasonic wave characteristics of nanorods", *Physica E* **42**:5 (2010), 1601–1604.

[Narendar and Gopalakrishnan 2010b] S. Narendar and S. Gopalakrishnan, "Terahertz wave characteristics of a single-walled carbon nanotube containing a fluid flow using the nonlocal Timoshenko beam model", *Physica E* **42**:5 (2010), 1706–1712.

[Narendar and Gopalakrishnan 2010c] S. Narendar and S. Gopalakrishnan, "Theoretical estimation of length dependent in-plane stiffness of single walled carbon nanotubes using the nonlocal elasticity theory", *J. Comput. Theor. Nanosci.* **7**:11 (2010), 2349–2354.

[Narendar and Gopalakrishnan 2010d] S. Narendar and S. Gopalakrishnan, "Ultrasonic wave characteristics of nanorods via nonlocal strain gradient models", *J. Appl. Phys.* **107**:8 (2010), Article ID #084312.

[Narendar et al. 2010] S. Narendar, D. R. Mahapatra, and S. Gopalakrishnan, "Investigation of the effect of nonlocal scale on ultrasonic wave dispersion characteristics of a monolayer graphene", *Comput. Mater. Sci.* **49**:4 (2010), 734–742.

[Novoselov et al. 2004] K. S. Novoselov, A. K. Geim, S. V. Morozov, D. Jiang, Y. Zhang, S. V. Dubonos, I. V. Grigorieva, and A. A. Firsov, "Electric field effect in atomically thin carbon films", *Science* **306**:5696 (2004), 666–669.

[Obraztsov et al. 2007] A. N. Obraztsov, E. A. Obraztsova, A. V. Tyurnina, and A. A. Zolotukhin, "Chemical vapor deposition of thin graphite films of nanometer thickness", *Carbon* **45**:10 (2007), 2017–2021.

[Ohta et al. 2006] T. Ohta, A. Bostwick, T. Seyller, K. Horn, and E. Rotenberg, "Controlling the electronic structure of bilayer graphene", *Science* **313**:5789 (2006), 951–954.

[Oshima and Nagashima 1997] C. Oshima and A. Nagashima, "Ultra-thin epitaxial films of graphite and hexagonal boron nitride on solid surfaces", *J. Phys. Condens. Matter* **9**:1 (1997), 1–20.

[Peddieson et al. 2003] J. Peddieson, G. R. Buchanan, and R. P. McNitt, "Application of nonlocal continuum models to nanotechnology", *Int. J. Eng. Sci.* **41**:3–5 (2003), 305–312.

[Reddy 2007] J. N. Reddy, "Nonlocal theories for bending, buckling and vibration of beams", *Int. J. Eng. Sci.* **45**:2–8 (2007), 288–307.

[Reddy and Pang 2008] J. N. Reddy and S. D. Pang, "Nonlocal continuum theories of beams for the analysis of carbon nanotubes", *J. Appl. Phys.* **103**:2 (2008), Article ID #023511.

[Sakhaee-Pour and Ahmadian 2008] A. Sakhaee-Pour and M. T. Ahmadian, "Potential application of single-layered graphene sheet as strain sensor", *Solid State Comm.* **147**:7–8 (2008), 336–340.

[Sakhaee-Pour et al. 2008a] A. Sakhaee-Pour, M. T. Ahmadian, and R. Naghdabadi, "Vibrational analysis of single-layered graphene sheets", *Nanotechnology* **19**:8 (2008), Article ID #085702.

[Sakhaee-Pour et al. 2008b] A. Sakhaee-Pour, M. T. Ahmadian, and A. Vafai, "Applications of single-layered graphene sheets as mass sensors and atomistic dust detectors", *Solid State Comm.* **145**:4 (2008), 168–172.

[Senturia 2001] S. D. Senturia, *Microsystem design*, Kluwer, Boston, 2001.

[Tomanek and Enbody 2000] D. Tomanek and R. Enbody, *Science and application of nanotubes*, Kluwer/Plenum, New York, 2000.

[Tounsi et al. 2008] A. Tounsi, H. Heireche, H. M. Berrabah, A. Benzair, and L. Boumia, "Effect of small size on wave propagation in double-walled carbon nanotubes under temperature field", *J. Appl. Phys.* **104**:10 (2008), Article ID #104301.

[Vossen and Kern 1978] J. L. Vossen and W. Kern, *Thin film processes*, Academic Press, New York, 1978.

[Wang 2005] Q. Wang, "Wave propagation in carbon nanotubes via nonlocal continuum mechanics", *J. Appl. Phys.* **98**:12 (2005), Article ID #124301.

[Wang and Duan 2008] C. M. Wang and W. H. Duan, "Free vibration of nanorings/arches based on nonlocal elasticity", *J. Appl. Phys.* **104**:1 (2008), Article ID #014303.

[Wang and Hu 2005] L. Wang and H. Hu, "Flexural wave propagation in single-walled carbon nanotubes", *Phys. Rev. B* **71**:19 (2005), Article ID #195412.

[Wang and Liew 2007] Q. Wang and K. M. Liew, "Application of nonlocal continuum mechanics to static analysis of micro- and nano-structures", *Phys. Lett. A* **363**:3 (2007), 236–242.

[Yakobson et al. 1997] B. I. Yakobson, M. P. Campbell, C. J. Brabec, and J. Bernholc, "High strain rate fracture and C-chain unraveling in carbon nanotubes", *Comput. Mater. Sci.* **8**:4 (1997), 341–348.

[Yang et al. 2002] F. Yang, A. C. M. Chong, D. C. C. Lam, and P. Tong, "Couple stress based strain gradient theory for elasticity", *Int. J. Solids Struct.* **39**:10 (2002), 2731–2743.

[Yang et al. 2008] J. Yang, X. L. Jia, and S. Kitipornchai, "Pull-in instability of nano-switches using nonlocal elasticity theory", *J. Phys. D Appl. Phys.* **41**:3 (2008), Article ID #035103.

[Zhou and Li 2001] S. J. Zhou and Z. Q. Li, *J. Shandong Univ. Technol.* **31** (2001), 401–407.

SAGGAM NARENDAR: snarendar@aero.iisc.ernet.in
Defence Research and Development Laboratory, Kanchanbagh, Hyderabad 500 058, India

SRINIVASAN GOPALAKRISHNAN: krishnan@aero.iisc.ernet.in
Department of Aerospace Engineering, Indian Institute of Science, Bangalore 560 012, India
http://www.aero.iisc.ernet.in/krishnan

JOURNAL OF MECHANICS OF MATERIALS AND STRUCTURES

jomms.net

Founded by Charles R. Steele and Marie-Louise Steele

Cover design: Alex Scorpan   Cover photo: Wikimedia Commons

See http://jomms.net for submission guidelines.